Direct Observation of the Mesopores in ZSM-5 Zeolites with Hierarchical Porous Structures by Laser-Hyperpolarized 129 Xe NMR

8 AUTHORS, INCLUDING:

Zhicheng Liu

35 PUBLICATIONS 799 CITATIONS

Shutao Xu

Chinese Academy of Sciences

57 PUBLICATIONS 519 CITATIONS

Zaiku Xie

China Petroleum and Chemical Corporation

82 PUBLICATIONS 1,371 CITATIONS

Direct Observation of the Mesopores in ZSM-5 Zeolites with Hierarchical Porous Structures by Laser-Hyperpolarized ^{129}Xe NMR

Yong Liu,[†] **Weiping Zhang,***[†] **Zhicheng Liu,**[‡] **Shutao Xu,**[†] **Yangdong Wang,**[‡] **Zaiku Xie,**[‡] **Xiuwen Han,**[†] **and Xinhe Bao***[,†]

State Key Laboratory of Catalysis, Dalian Institute of Chemical Physics, Chinese Academy of Sciences, 457 Zhongshan Road, Dalian 116023, China, and SINOPEC Shanghai Research Institute of Petrochemical Technology, 1658 Pudong Beilu, Shanghai 201208, China

Received: April 1, 2008; Revised Manuscript Received: June 10, 2008

Mesopore-modified ZSM-5 zeolites with hierarchical porous structures (Meso-ZSM-5) have been synthesized by using tetrapropylammonium hydroxide and starch as cotemplates. One- and two-dimensional ^{129}Xe NMR spectroscopy has been employed to study the porosity under the continuous flow of laser-hyperpolarized xenon gas. Besides the micropores, the mesoporous domains in Meso-ZSM-5 zeolites are directly observed by variable-temperature experiments. Combining with nitrogen adsorption, the influence of the Si/Al ratios on the mesopores in Meso-ZSM-5 is also investigated. The exchange of Xe atoms in different types of pores is very fast at ambient temperature. Two-dimensional exchange spectroscopy (EXSY) is used for the first time to monitor such an exchange process, and the results indicate that even at very low temperature Xe atoms still undergo much faster exchange between mesopores and micropores in Meso-ZSM-5 than in the mechanical mixture of conventional ZSM-5 and mesoporous silica. The results demonstrate that these hierarchical pores may have good connected networks that facilitate xenon diffusion and exchange. Also, this may give some indications for other molecules adsorption and diffusion in mesoporous zeolites especially in the process of catalysis.

1. Introduction

Zeolites based on uniform microporous pores in the molecular dimension have found wide applications in chemical industry.[1,2] However, the catalytic activity of zeolites is often limited by the diffusion of reagents and reaction products through the framework pore network due to the small channels and cavities (typically smaller than 1.2 nm).[3] Recently, the materials with hierarchical porosity have aroused great interests in both synthesis and catalytic applications, as they can combine the advantages of microporous zeolites with high activity and stability and mesoporous materials with large pore size.[4–10] Several efforts have been made to synthesize micro-/mesoporous composite zeolites by partial desilication,[5] recrystallizing the walls of the mesoporous materials,[6] assembling the zeolite precursors, seeds, or nanoparticles as building blocks, adding polymers, or using functional organosilica, etc.[7–9] The promising mesopore-modified zeolites with fully crystalline walls and intracrystal mesopores can be obtained by adding soft or hard templates during the synthesis and then removing these scaffolds.[10,11] One of our previous studies shows that nanosized CaCO$_3$ as hard template is a useful approach for creation of intracrystal pores.[11c]

The porous structures are crucial and decisive for molecule diffusion processes and the shape selectivities in catalytic reactions. These hierarchical porous zeolites have already shown the improved performances in various hydrocarbon conversions such as cracking and isomerization of alkanes,[10c] alkylation of aromatics,[12] and some cases in environmental catalysis.[13] The benefits of introduced mesopores have been attributed to the improved mass transport to and from the active sites located in the micropores of zeolites.[11–14] However, the direct demonstrations of such enhanced diffusion and the textural porosity of these composite zeolites have not been well established in the literature so far. Normally, N$_2$ adsorption is of the first choice to study the porous texture of the materials and the changes therein upon post-treatments. Yet the ideal models present the limited network effects and poor descriptions of the geometrical and energetic effects of the pores as well as the wall surfaces.[15,16] Although the advanced high-resolution transmission electron microscopy provides the direct method for charactering the fine structures, the inferred partial and local information may be misleading at some times and cannot represent the whole picture, and there are disadvantages for the study of the electron-beam-sensitive zeolites.[17]

^{129}Xe NMR spectroscopy is a powerful tool for probing the porosity and species distribution in porous materials.[18] The optical pumping by laser for the production of hyperpolarized (HP) xenon facilitate it working at very low concentration of xenon (∼1%) under continuous flow.[19] The observed ^{129}Xe chemical shift could reflect mainly interactions between xenon atoms and the surface. Xe is also very sensitive to the geometry and may represent the connectivity and uniformity of the pores. Our study and other studies show that this technique is very attractive for materials analysis.[20–22] Moreover, HP ^{129}Xe NMR two-dimensional exchange spectroscopy (EXSY) is able to monitor microscopic motions of Xe atoms between different porous environments.[20f,23] Therefore, laser-hyperpolarized ^{129}Xe NMR is a sensitive and direct tool to explore the porosity of such materials with hierarchical pores and has the potential to reveal textural connectivity as well as the dynamics of adsorbed Xe therein.

* Corresponding author. Phone: +86-411-8437 9976. Fax: +86-411-8469 4447. E-mail: wpzhang@dicp.ac.cn (W.Z.); xhbao@dicp.ac.cn (X.B.).
† Chinese Academy of Sciences.
‡ SINOPEC Shanghai Research Institute of Petrochemical Technology.

In the present work, Meso-ZSM-5 zeolites with hierarchical pores have been synthesized by using starch as cheap templates. Continuous-flow hyperpolarized ^{129}Xe NMR has been employed to study the porous structure by variable-temperature experiments. Combining with nitrogen sorption, the influence of the Si/Al ratio on the mesopore size distributions as well as the mesoporous volumes of Meso-ZSM-5 has been discussed. For comparison, the porosities of pure-phased ZSM-5, porous silica, and their mechanical mixture are also investigated. Two-dimensional (2D) exchange NMR experiments are used to illustrate the exchange process of xenon in Meso-ZSM-5 and in the physical mixture counterparts to reveal their porous structure differences.

2. Experimental Section

2.1. Sample Preparation and Characterization. Meso-ZSM-5 with Si/Al ratios of 100, 50, and 25 (Meso-ZSM-5-n, where n denotes the Si/Al ratio) were synthesized by adding starch into the gel of the ZSM-5 with the typical composition of $200SiO_2$:xAl_2O_3:$40-160$TPAOH:$6000-20\,000H_2O$:0.05 starch, where $x = 1$, 2, and 4, respectively. ZSM-5 with an Si/Al ratio of 50 was synthesized by the same method using tetrapropylammonium hydroxide (TPAOH) as the template but without adding starch. After aging, the gel was transferred into a Teflon-lined stainless-steel autoclave and kept at a desired temperature for a few days. After crystallization, all samples were thoroughly washed with deionized water, dried at 353 K, and then calcined at 823 K in air for 7 h. Mesoporous silica with the same mesopore size was purchased from BASF AG, Germany. The weight ratio of ZSM-5 and silica in mechanically mixed sample was 2:1, and the two parts were blended thoroughly. The crystalline phases of these samples were confirmed by XRD patterns obtained at room temperature on a Rigaku D/max-rb diffractometer with Cu Kα radiation, and the relative crystallinity of zeolites was calculated on the basis of the intensity of the peaks of angle $2\theta = 22-25°$ in the patterns.[24] The nitrogen adsorption and desorption isotherms were measured at 77 K on a Quantachrome Autosobe-1 physical adsorption apparatus. All samples were outgassed at 573 K overnight before measurements.

2.2. Continuous-Flow Hyperpolarized ^{129}Xe NMR. Laser-hyperpolarized (HP) ^{129}Xe NMR experiments were carried out at 110.6 MHz on the Varian Infinity-plus 400 spectrometer using a 7.5 mm probe. Prior to each experiment, samples were pressed, crushed, and sieved into $20-40$ mesh particles, then dehydrated at 673 K under vacuum ($<10^{-5}$ Torr) for ca. 20 h. Optical polarization of xenon was achieved with a homemade apparatus as reported in our previous study,[20d−f] with the optical pumping cell in the fringe field of the spectrometer magnet and 60 W diode laser array (Coherent FAP-System). A flow of 1% Xe−1% N_2−98% He gas mixture was delivered at the rate of $200-250$ mL/min to the sample in detection region via plastic tubing. Variable-temperature NMR measurements were performed in the range of $138-298$ K. All one-dimensional spectra were acquired with 3.0 μs π/2 pulse, $100-200$ scans, and 2 s recycle delay. The chemical shifts were referenced to the signal of xenon gas. Although the line of the xenon gas is temperature dependence, generally chemical shifts vary no more than 1 ppm in the temperature range of the experiments. The two-dimensional exchange experiments (2D-EXSY) were performed at 143 K using a $90°-t_1-90°-\tau_m-90°-t_2$ pulse sequence in TPPI mode. Each 2D spectrum was acquired with 32 points in the t_1 dimension and 1024 points in the t_2 dimension. Before Fourier transformation, the t_1 dimension was zero-filled to 256 points. Mixing times were varied from 0.1 to 10 ms.
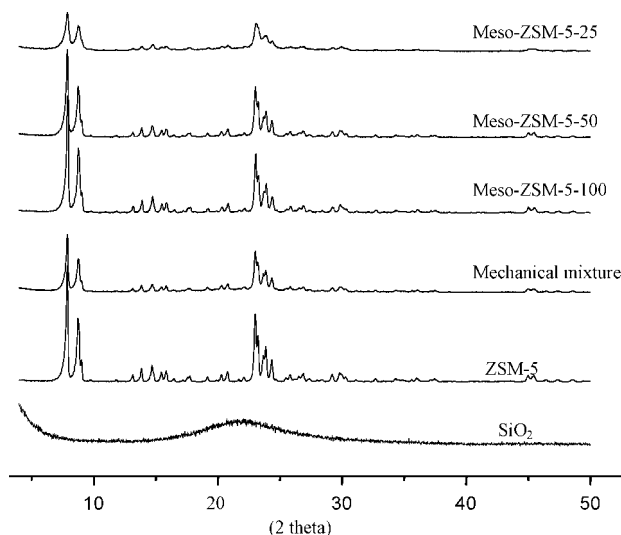

Figure 1. XRD patterns of Meso-ZSM-5 with Si/Al ratios of 25, 50, and 100, respectively, as well as conventional ZSM-5, silica, and the mechanical mixture of conventional ZSM-5 and silica. All of the patterns were collected at room temperature on a Rigaku D/max-rb diffractometer in a 2θ range of $4-50°$.

TABLE 1: Pore Structural Parameters and Relative Crystallinities of Meso-ZSM-5 with Si/Al Ratios of 25, 50, and 100 as Well as Conventional ZSM-5, Silica, and Their Mechanical Mixture

sample	Si/Al	relative crystallinity (%)	V_{micro} (cm^3/g)^a	V_{meso} (cm^3/g)^b	BET surface area (cm^2/g)^c
Meso-ZSM-5	25	75	0.10	0.44	375
Meso-ZSM-5	50	87	0.10	0.34	373
Meso-ZSM-5	100	91	0.11	0.14	367
ZSM-5	50	100	0.16		375
mixture		70	0.10	0.30	350
SiO$_2$			0.02	1.1	244

^{a} Calculated by *t*-plot method. ^{b} Calculated by BJH model from the desorption curve. ^{c} Calculated by multipoint BET method.

3. Results and Discussion

3.1. XRD and Nitrogen Adsorption. As shown in Figure 1, the XRD pattern of ZSM-5 is consistent with that reported in the literature,[24] and the patterns of Meso-ZSM-5 also agree well with that of the conventional ZSM-5. Except for Meso-ZSM-5 with an Si/Al ratio of 25, the other two samples with higher Si/Al ratios have high crystallinity. The apparent relative crystallinity (taking the crystallinity of conventional ZSM-5 as 100%) decreases with increasing the aluminum concentration, as listed in Table 1. The high content of aluminum may inhibit the crystallization of Meso-ZSM-5 when adding starch as the template. Figure 2 shows the nitrogen physisorption isotherms, and the inset is the corresponding BJH mesopore size distribution. For Meso-ZSM-5, the N_2 adsorption and desorption curves exhibit type-IV isotherm with a steep increase at relative pressures $P/P_0 < 0.02$ and a hysteresis loop above $P/P_0 = 0.4$. These adsorptions are interpreted as micropores filling and capillary condensation in mesopores, respectively.[10c] The mesopore sizes of Meso-ZSM-5 with Si/Al ratios of 25 and 50 are distributed in the range of $10-30$ nm and centered at ca. 20 nm, while the mesopore in Meso-ZSM-5 with Si/Al ratio of 100 is not obvious. The surface areas as well as micropore and mesopore volumes are summarized in Table 1. The mesopore volumes increase with decreasing the Si/Al ratios, while the surface areas and micropore volumes change in a minor way. From Figure 1, we also know that Meso-ZSM-5-50 and the
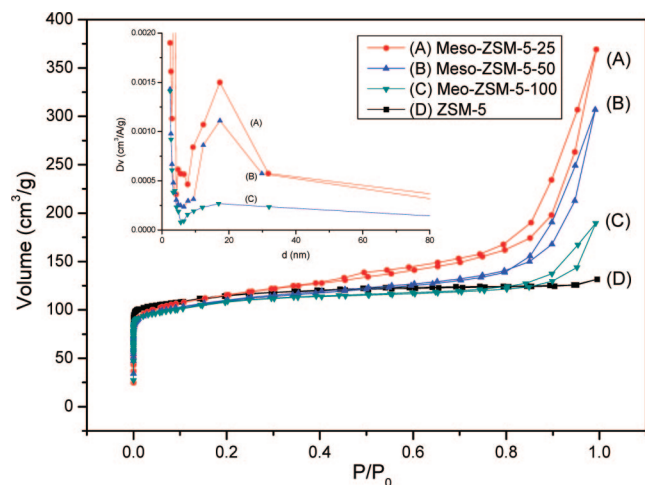
Figure 2. Nitrogen adsorption/desorption isotherms of Meso-ZSM-5 with Si/Al ratios of 25, 50, 100 and conventional ZSM-5 zeolites at 77 K, and the inset shows the mesopore size distribution of Meso-ZSM-5 calculated by BJH model from the desorption curve.
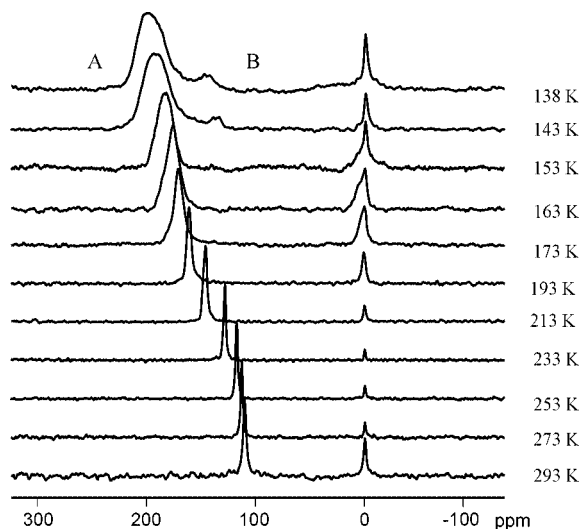

Figure 4. Laser-hyperpolarized ^{129}Xe NMR spectra of Xe adsorbed in Meso-ZSM-5 with Si/Al ratio of 50. The temperature is varied from 293 to 138 K. The spectra were acquired in a static state with 3.0 μs π/2 pulse, 100–200 scans, and 2 s recycle delay.

Figure 3. Laser-hyperpolarized ^{129}Xe NMR spectra of Xe adsorbed in Meso-ZSM-5 with Si/Al ratio of 25. The temperature is varied from 293 to 138 K. The spectra were acquired in a static state with 3.0 μs π/2 pulse, 100–200 scans, and 2 s recycle delay.

Figure 5. Laser-hyperpolarized ^{129}Xe NMR spectra of Xe adsorbed in Meso-ZSM-5 with Si/Al ratio of 100. The temperature is varied from 293 to 138 K. The spectra were acquired in a static state with 3.0 μs π/2 pulse, 100–200 scans, and 2 s recycle delay.

mechanically mixed sample (ZSM-5/SiO$_2$) show similar diffractions in XRD patterns. Meanwhile, their nitrogen adsorption isotherms are analogous, and their surface areas as well as pore volumes show no big difference (see Table 1). So it cannot get any valuable information from the routine XRD and nitrogen adsorption measurements to distinguish mesoporous zeolites and mechanically mixed zeolite/silica counterparts.

3.2. HP ^{129}Xe NMR of Meso-ZSM-5 with Different Si/Al Ratios. The variable-temperature laser-hyperpolarized (HP) ^{129}Xe NMR spectra of Meso-ZSM-5 with different Si/Al ratios are shown in Figures 3–5. The peaks at 0 ppm in all spectra are from xenon in the gas phase. From 293 to 153 K, there is only one downfield signal A, which may originate from the adsorbed xenon in zeolites. The chemical shifts of the line from Xe in zeolites increase when the temperature decreases from 293 to 143 K. It is a general trend in variable-temperature ^{129}Xe NMR experiments for porous materials mainly due to the increase of the Xe-surface as well as Xe–Xe interactions at lower temperatures. At 143 K, a new upfield line B emerges for Meso-ZSM-5-25 (Figure 3) and Meso-ZSM-5-50 (Figure 4) and shifts downfield with decreasing temperature. This means
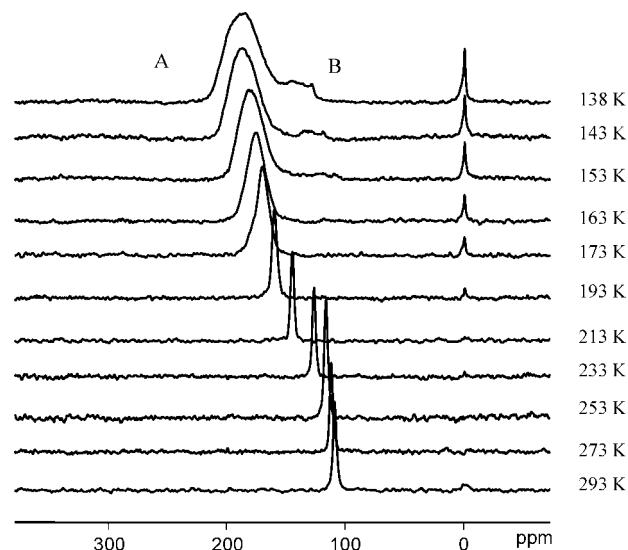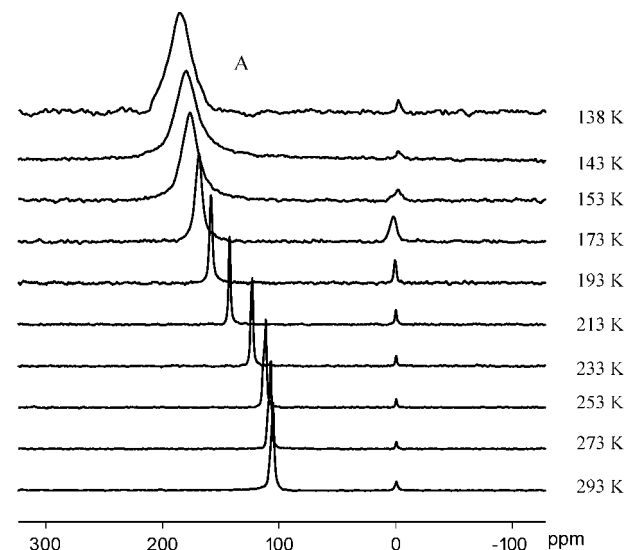
that there is more than one type of pore distribution environment in the Meso-ZSM-5 zeolites with Si/Al ratios of 25 and 50, and the fast exchange of Xe among these pores exists above 153 K. For comparison, the variable-temperature HP ^{129}Xe NMR spectra of Xe adsorbed in conventional ZSM-5 with an Si/Al ratio of 50 are shown in the Supporting Information (Figure S1), and the chemical shift variations with temperature of all samples are also shown in Figure S2. There is only one line ascribed to Xe adsorbed in the channels, that is, micropores of ZSM-5 in Figure S1. The temperature-dependent behavior of line A in Figures 3–5 is similar to that of conventional ZSM-5. Figure 6 shows the laser-hyperpolarized (HP)^{129}Xe NMR spectra of Meso-ZSM-5 with different Si/Al ratios and conventional ZSM-5 at 293 and 143 K, respectively. Obviously, as indicated in Figure 6, the downfield signal A with much stronger intensities in the spectra of Meso-ZSM-5 should be assigned to Xe adsorbed in the micropores of Meso-ZSM-5. The new upfield line B when decreasing the temperature to 143
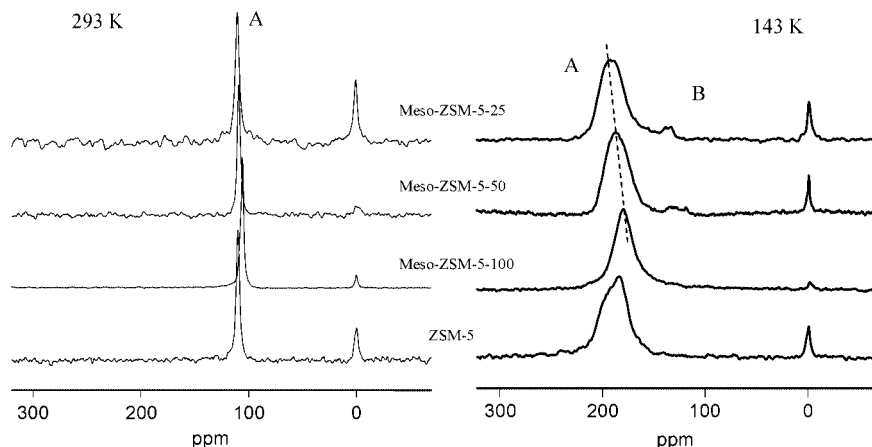
Figure 6. Laser-hyperpolarized [129]Xe NMR spectra of Xe adsorbed in Meso-ZSM-5 with Si/Al ratios of 25, 50, 100, respectively, and conventional ZSM-5 zeolites at temperatures of 293 and 143 K.

K may come from Xe adsorbed in the mesopores of Meso-ZSM-5. The nearly overlapped two peaks in the mesoporous region may indicate the relatively broad distribution of mesopores in Meso-ZSM-5. The peak area of signal A is larger than that of signal B. This can be due to the preferential adsorption of xenon in the micropores rather than in the mesopores at lower temperatures. From Figure 6 we can see that line A shifts downfield with decreasing Si/Al ratio in the Meso-ZSM-5. As pointed out by Chen and Zhang et al.,[25] the chemical shifts of adsorbed Xe depend on the chemical composition of the zeolite surface, that is, the aluminum content in the present case. So, the largest chemical shift of Xe absorbed in the microprous channels of Meso-ZSM-5 comes from the sample with an Si/Al ratio of 25. Also, this influence may also exist in line B from the mesopores. One can see that line B in Meso-ZSM-5-25 shows a relatively larger chemical shift than that in the Meso-ZSM-5-50, although their mesopore size distribution is similar. Besides the chemical shift, there is also obvious change in the line-shape of signal A when decreasing the temperature, which is probably due to the chemical shift anisotropy. Line B in Meso-ZSM-5-50 is broader than that in the Meso-ZSM-5-25. The origin may be probably due to the former containing more different pore environments for Xe. Surprisingly, there is no obvious signal of Xe adsorbed in the mesopores of Meso-ZSM-5-100 during the entire temperature range in the spectra (see Figure 5). It may be not unexpected if considering the nitrogen adsorption results (see Figure 2 and Table 1).

From the above results, we know that the Si/Al ratio of Meso-ZSM-5 has great influence on the mesopore size distribution and the mesopore volumes. With incorporating more aluminum species, Meso-ZSM-5 may possess more uniform mesopores and larger mesopore volumes.

3.3. HP [129]Xe NMR of Meso-ZSM-5 and Mechanically Mixed ZSM-5/Silica Counterparts. To get a better understanding of the porous structure in Meso-ZSM-5, we prepared a mechanical mixture of conventional ZSM-5 with an Si/Al ratio of 50 and porous silica with mesopore size and volume similar to those in the Meso-ZSM-5. Figure 7 shows the VT HP [129]Xe NMR spectra of mechanically mixed ZSM-5 and silica samples. At room temperature, there is nearly a single line, which may be assigned to Xe adsorbed in micropores of conventional ZSM-5. When the temperature decreases to 173 K and even lower, an additional upfield peak becomes much more obvious as compared to Meso-ZSM-5-50, which indicates that there are two types of pores in the mechanical mixture. For a better understanding of the porous structure in Meso-ZSM-5 zeolites,
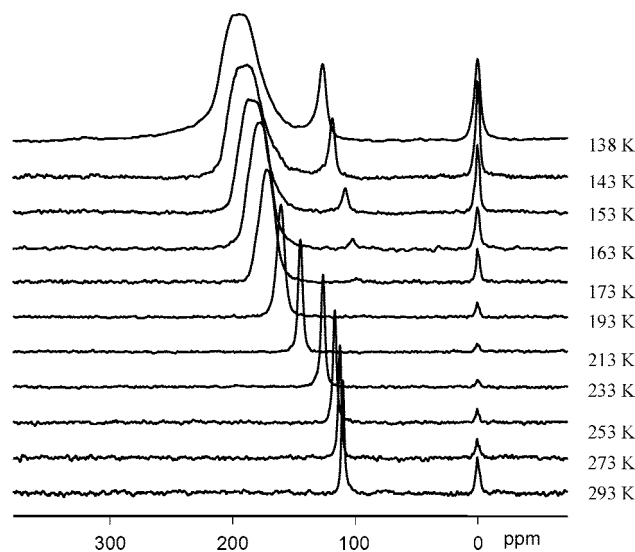

Figure 7. Temperature-dependent laser-hyperpolarized [129]Xe NMR spectra of Xe adsorbed in a mechanical mixture of silica and conventional ZSM-5. The temperature is varied from 293 to 138 K. The spectra were acquired in a static state with 3.0 μs $\pi/2$ pulse, 100−200 scans, and 2 s recycle delay.
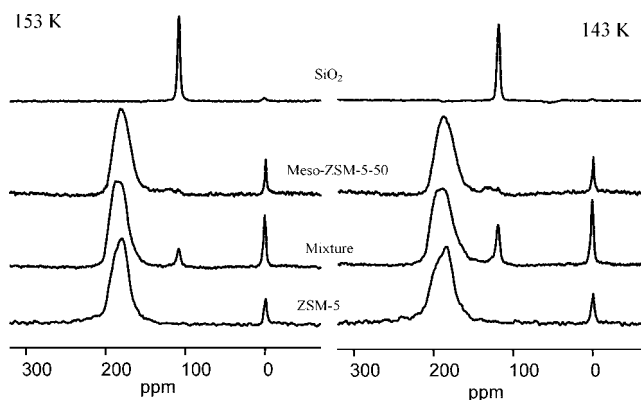

Figure 8. Laser-hyperpolarized [129]Xe NMR spectra of Xe adsorbed in Meso-ZSM-5-50, conventional ZSM-5, silica, and mechanical mixture at 153 and 143 K.

Figure 8 shows the HP [129]Xe NMR spectra of Meso-ZSM-5 and mechanically mixed ZSM-5/silica counterparts as well as the reference samples, conventional ZSM-5 and silica at 153 and 143 K, respectively. The exchange of Xe atoms in different pores of the individual material is slow at such low temperatures,
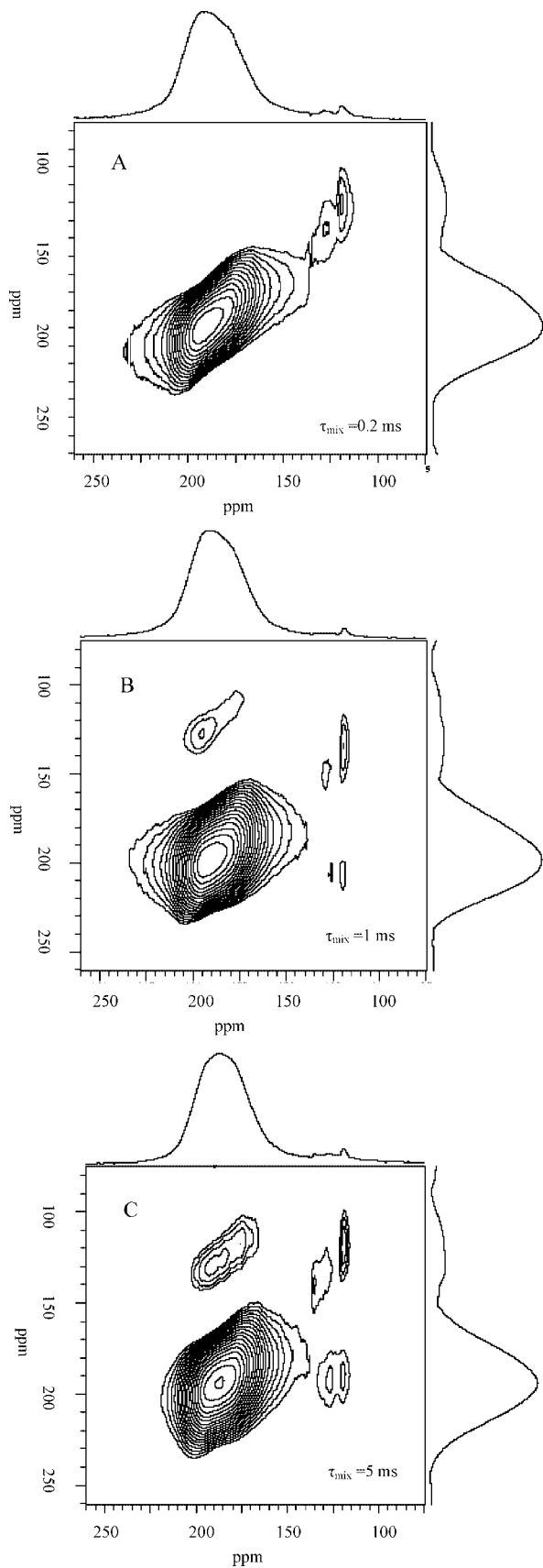
Direct Observation of the Mesopores in ZSM-5 Zeolites

J. Phys. Chem. C, Vol. 112, No. 39, 2008 **15379**

Figure 9. Laser-hyperpolarized ^{129}Xe 2D-EXSY NMR spectra of Meso-ZSM-5-50 at 143 K with different mixing times: (A) $\tau_{mix} = 0.2$ ms; (B) $\tau_{mix} = 1$ ms; (C) $\tau_{mix} = 5$ ms using a $90°-t_1-90°-\tau_m-90°-t_2$ pulse sequence in TPPI mode. Each 2D spectrum was acquired with 32 points in the t_1 dimension and 1024 points in the t_2 dimension. Before Fourier transformation, the t_1 dimension was zero-filled to 256 points.
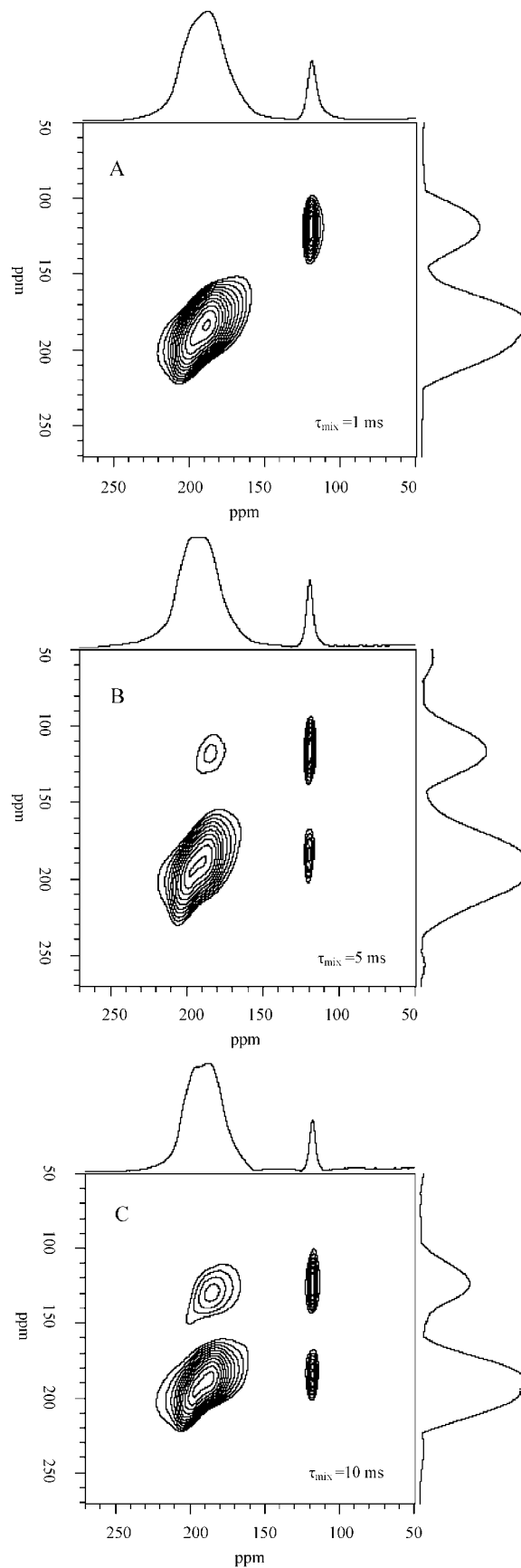
Figure 10. Laser-hyperpolarized ^{129}Xe 2D-EXSY NMR spectra of mechanically mixed conventional ZSM-5 and silica at 143 K with different mixing times: (A) $\tau_{mix} = 1$ ms; (B) $\tau_{mix} = 5$ ms; (C) $\tau_{mix} = 10$ ms. Each 2D spectrum was acquired with 32 points in the t_1 dimension and 1024 points in the t_2 dimension. Before Fourier transformation, the t_1 dimension was zero-filled to 256 points.

so the signals in the ^{129}Xe NMR spectra of mechanical mixture may represent the characteristic structure of zeolite ZSM-5 and porous silica, respectively. It can be seen from Figure 8 that the downfield signal should come from Xe in the micropores of ZSM-5, while the upfield line should be ascribed to Xe adsorbed in the mesopores. At 143 K, the chemical shift difference ($\Delta\delta$) of xenon in these two domains is 56 ppm for the Meso-ZSM-5 zeolites, which is less than that of 70 ppm for the mechanically mixed ones. The results show that Xe exchange may be faster between micropores and mesopores in the Meso-ZSM-5 zeolites than in the mechanically mixed counterparts, which may also demonstrate the connectivity of these two pores is different. Similar phenomena have also been found by Liu et al. in the characterization of mesoporous/microporous composite materials by ^{129}Xe NMR.[26] The exchange rate of Xe atoms between Al-MCM-41 (or Al-SBA-15) and ZSM-5 is lower in the mechanical mixture than in the corresponding composite mesoporous materials. In the spectra of Meso-ZSM-5-50, the line of Xe in mesopores is much broader than that in the mechanical mixture. The origin may be also due to the mesopore size distribution difference. Meso-ZSM-5-50 may possess less uniform mesopores than the ZSM-5/silica mechanical mixture.

3.4. HP ^{129}Xe Two-Dimensional Exchange Spectra. A powerful tool for the study of exchange process is 2D-exchange NMR spectroscopy (EXSY). The technique can be extended to study the dynamic processes of adsorbed Xe in porous solid materials.[27] 2D EXSY is obtained by monitoring frequencies before and after a so-called mixing time, τ_{mix}, during which spin exchange and/or molecular reorientation motions can occur. Changes in the NMR frequencies manifest themselves as off-diagonal intensities in a 2D exchange spectrum, which depends on the mixing time. The cross-peaks indicate an exchange of xenon atoms between the corresponding environments on the diagonal within the period of τ_{mix}.[28] To see more clearly the exchange of adsorbed Xe atoms between these two different domains and how fast these exchange processes might be, HP ^{129}Xe 2D EXSY spectra were recorded at 143 K for Meso-ZSM-5-50 and mechanically mixed ZSM-5/silica counterparts, which are shown in Figures 9 and 10, respectively. The corresponding 1D projection is displayed above the EXSY for clarity. The absence of cross-peaks in Figure 9A demonstrates that the exchange between the micropores and mesopores in Meso-ZSM-5-50 does not occur during short exchange times $\tau_{mix} \leq 0.2$ ms. The presence of cross-peaks between two ^{129}Xe NMR peaks assigned to exchanging Xe between micropores and mesopores in Figure 9B suggests that the exchange of xenon between these environments exists at a time scale of 1 ms. The cross-peaks get more strong when increasing τ_{mix} to 5 ms. So, for Meso-ZSM-5-50, the Xe exchange takes place between these two types of porous domains at the time scale of less than 1 ms. There seem to be two peaks corresponding to the mesopores in the material as indicated by the three diagonal peaks in all three of the spectra. The small cross-peaks in Figure 9C at least indicate the exchange between these two mesopore peaks. We estimate that the Xe may undergo exchange between these pores considering some unclear cross-peaks. For the mechanically mixed sample, 2D exchange spectra show that there is no Xe exchanging between conventional ZSM-5 and silica at the τ_{mix} of 1 ms (Figure 10A). The xenon exchange emerges when τ_{mix} increases to 5 ms and becomes rapid for the appearance of strong cross-peaks when τ_{mix} increases further to 10 ms (Figure 10B,C). So, for the mechanical mixture, the Xe exchange occurs when the mixing time close to 5 ms. It is the interparticle diffusion

of Xe between these two domains, which could be slower than that in Meso-ZSM-5-50. This reveals that the microporous and mesoporous domains in the Meso-ZSM-5 may stay much closer and have better connectivity than that in the physical mixture. The incorporated connected mesopores may be responsible for the enhanced diffusion of Xe through the crystals. The result may also give some indications for other molecules adsorption and diffusion in mesoporous zeolites especially in the process of catalysis.

4. Conclusions

The porous structures of mesopore-modified ZSM-5 zeolites have been studied by continuous-flow laser-hyperpolarized ^{129}Xe NMR. Different adsorption domains of Xe in these hierarchical porous zeolites can be directly observed by variable-temperature experiments. The exchange of Xe atoms in different types of pore environments is very fast at ambient temperatures. Combining with nitrogen physisorption, we found that the Si/Al ratios of resultant samples have great influence on the mesopore size distribution and mesopore volume in Meso-ZSM-5. The two-dimensional exchange NMR spectroscopy (EXSY) has been used for the first time on such hierarchical zeolites, and the results show that Xe atoms still undergo faster exchange between different types of pores in the Meso-ZSM-5 than in the mechanically mixed ZSM-5/silica counterparts even at very low temperature. The results demonstrate that microporous and mesoporous domains in the Meso-ZSM-5 may stay much closer and have better connectivity than in the conventional physical mixture, which facilitate the Xe atoms diffusion and exchange.

Supporting Information Available: Variable-temperature hyperpolarized ^{129}Xe NMR spectra of conventional ZSM-5. Temperature-dependent chemical shifts of Xe and ^{27}Al MAS NMR spectra of all samples. This material is available free of charge via the Internet at http://pubs.acs.org.

References and Notes

(1) Corma, A. *Chem. Rev.* **1995**, *95*, 559.
(2) Cundy, C. S.; Cox, P. A. *Chem. Rev.* **2003**, *103*, 663.
(3) (a) van Donk, S.; Janssen, A. H.; Bitter, J. H.; de Jong, K. P. *Catal. Rev.-Sci. Eng.* **2003**, *45*, 297. (b) Cejka, J.; Mintova, S. *Catal. Rev.-Sci. Eng.* **2007**, *49*, 457.
(4) Hartmann, M. *Angew. Chem., Int. Ed.* **2004**, *43*, 5880. (b) Tao, Y. S.; Kanoh, H.; Abrams, L.; Kaneko, K. *Chem. Rev.* **2006**, *106*, 896.
(5) (a) Groen, J. C.; Moulijn, J. A.; Perez-Ramirez, J. *Microporous Mesoporous Mater.* **2005**, *87*, 153. (b) Groen, J. C.; Moulijn, J. A.; Perez-Ramirez, J. *J. Mater. Chem.* **2006**, *16*, 2121.
(6) (a) Kloetstra, K. R.; vanBekkum, H.; Jansen, J. C. *Chem. Commun.* **1997**, 2281. (b) Guo, W. P.; Huang, L. M.; Deng, P.; Xue, Z. Y.; Li, Q. Z. *Microporous Mesoporous Mater.* **2001**, *44*, 427. (c) On, D. T.; Kaliaguine, S. *Angew. Chem., Int. Ed.* **2001**, *40*, 3248.
(7) Karlsson, A.; Stocker, M.; Schmidt, R. *Microporous Mesoporous Mater.* **1999**, *27*, 181.
(8) (a) Liu, Y.; Zhang, W. Z.; Pinnavaia, T. J. *Angew. Chem., Int. Ed.* **2001**, *40*, 1255. (b) Zhang, Z. T.; Han, Y.; Xiao, F. S.; Qiu, S. L.; Zhu, L.; Wang, R. W.; Yu, Y.; Zhang, Z.; Zou, B. S.; Wang, Y. Q.; Sun, H. P.; Zhao, D. Y.; Wei, Y. *J. Am. Chem. Soc.* **2001**, *123*, 5014.
(9) (a) Wang, H.; Pinnavaia, T. J. *Angew. Chem., Int. Ed.* **2006**, *45*, 7603. (b) Xiao, F. S.; Wang, L. F.; Yin, C. Y.; Lin, K. F.; Di, Y.; Li, J. X.; Xu, R. R.; Su, D. S.; Schlogl, R.; Yokoi, T.; Tatsumi, T. *Angew. Chem.,*

Direct Observation of the Mesopores in ZSM-5 Zeolites

J. Phys. Chem. C, Vol. 112, No. 39, 2008 **15381**

Int. Ed. **2006**, *45*, 3090. (c) Choi, M.; Cho, H. S.; Srivastava, R.; Venkatesan, C.; Choi, D. H.; Ryoo, R. *Nat. Mater.* **2006**, *5*, 718.

(10) (a) Yang, Z. X.; Xia, Y. D.; Mokaya, R. *Adv. Mater.* **2004**, *16*, 727. (b) Fang, Y. M.; Hu, H. Q. *J. Am. Chem. Soc.* **2006**, *128*, 10636. (c) Ogura, M.; Zhang, Y. W.; Elangovan, S. P.; Okubo, T. *Microporous Mesoporous Mater.* **2007**, *101*, 224.

(11) (a) Jacobsen, C. J. H.; Madsen, C.; Houzvicka, J.; Schmidt, I.; Carlsson, A. *J. Am. Chem. Soc.* **2000**, *122*, 7116. (b) Kustova, M.; Egeblad, K.; Zhu, K.; Christensen, C. H. *Chem. Mater.* **2007**, *19*, 2915. (c) Zhu, H. B.; Liu, Z. C.; Wang, Y. D.; Kong, D. J.; Yuan, X. H.; Xie, Z. K. *Chem. Mater.* **2008**, *20*, 1134.

(12) (a) Groen, J. C.; Sano, T.; Moulijn, J. A.; Perez-Ramirez, J. *J. Catal.* **2007**, *251*, 21. (b) Christensen, C. H.; Johannsen, K.; Schmidt, I.; Christensen, C. H. *J. Am. Chem. Soc.* **2003**, *125*, 13370.

(13) (a) Groen, J. C.; Bruckner, A.; Berrier, E.; Maldonado, L.; Moulijn, J. A.; Perez-Ramirez, J. *J. Catal.* **2006**, *243*, 212. (b) Kustova, M. Y.; Rasmussen, S. B.; Kustov, A. L.; Christensen, C. H. *Appl. Catal., B* **2006**, *67*, 60.

(14) (a) Kortunov, P.; Vasenkov, S.; Karger, J.; Valiullin, R.; Gottschalk, P.; Elia, M. F.; Perez, M.; Stocker, M.; Drescher, B.; McElhiney, G.; Berger, C.; Glaser, R.; Weitkamp, J. *J. Am. Chem. Soc.* **2005**, *127*, 13055. (b) Christensen, C. H.; Johannsen, K.; Toernqvist, E.; Schmidt, I.; Topsoe, H.; Christensen, C. H. *Catal. Today* **2007**, *128*, 117. (c) Groen, J. C.; Zhu, W. D.; Brouwer, S.; Huynink, S. J.; Kapteijn, F.; Moulijn, J. A.; Perez-Ramirez, J. *J. Am. Chem. Soc.* **2007**, *129*, 355.

(15) Groen, J. C.; Peffer, L. A. A.; Perez-Ramirez, J. *Microporous Mesoporous Mater.* **2003**, *60*, 1.

(16) Leofanti, G.; Padovan, M.; Tozzola, G.; Venturelli, B. *Catal. Today* **1998**, *41*, 207.

(17) Terasaki, O.; Ohsuna, T. *Catal. Today* **1995**, *23*, 201.

(18) (a) Ito, T.; Fraissard, J. *J. Chem. Phys.* **1982**, *76*, 5225. (b) Ripmeester, J. A. *J. Am. Chem. Soc.* **1982**, *104*, 289. (c) Bonardet, J. L.; Fraissard, J.; Gédéon, A.; Springuel-Huet, M. A. *Catal. Rev.-Sci. Eng.* **1999**, *41*, 115. (d) Zhang, W. P.; Han, X. W.; Liu, X. C.; Lei, H.; Bao, X. H. *Chem. Commun.* **2001**, 293.

(19) Raftery, D.; MacNamara, E.; Fisher, G.; Rice, C. V.; Smith, J. *J. Am. Chem. Soc.* **1997**, *119*, 8746.

(20) (a) Moudrakovski, I. L.; Nossov, A.; Lang, S.; Breeze, S. R.; Ratcliffe, C. I.; Simard, B.; Santyr, G.; Ripmeester, J. A. *Chem. Mater.* **2000**, *12*, 1181. (b) Zhang, W. P.; Ratcliffe, C. I.; Moudrakovski, I. L.; Mou, C. Y.; Ripmeester, J. A. *Anal. Chem.* **2005**, *77*, 3379. (c) Huang, S. J.; Huang, C. H.; Chen, W. H.; Sun, X. P.; Zeng, X. Z.; Lee, H. K.;

Ripmeester, J. A.; Mou, C. Y.; Liu, S. B. *J. Phys. Chem. B* **2005**, *109*, 681. (d) Li, X. J.; Zhang, W. P.; Liu, S. L.; Han, X. W.; Xu, L. Y.; Bao, X. H. *J. Catal.* **2007**, *250*, 55. (e) Jin, C. Z.; Li, G.; Wang, X. S.; Zhao, L. X.; Liu, L. P.; Liu, H.; Liu, Y.; Zhang, W. P.; Han, X. W.; Bao, X. H. *Chem. Mater.* **2007**, *19*, 1664. (f) Liu, Y.; Zhang, W. P.; Xie, S. J.; Xu, L. Y.; Han, X. W.; Bao, X. H. *J. Phys. Chem. B* **2008**, *112*, 1226. (g) Liu, Y.; Zhang, W. P.; Han, X. W.; Bao, X. H. *Chin. J. Catal.* **2006**, *27*, 827.

(21) (a) Haake, M.; Pines, A.; Reimer, J. A.; Seydoux, R. *J. Am. Chem. Soc.* **1997**, *119*, 11711. (b) Meersmann, T.; Logan, J. W.; Simonutti, R.; Caldarelli, S.; Comotti, A.; Sozzani, P.; Kaiser, L. G.; Pines, A. *J. Phys. Chem. A* **2000**, *104*, 11665. (c) Kneller, J. M.; Soto, R. J.; Surber, S. E.; Colomer, J. F.; Fonseca, A.; Nagy, J. B.; Van Tendeloo, G.; Pietrass, T. *J. Am. Chem. Soc.* **2000**, *122*, 10591.

(22) (a) Nossov, A.; Haddad, E.; Guenneau, F.; Mignon, C.; Gédéon, A.; Grosso, D.; Babonneau, F.; Bonhomme, C.; Sanchez, C. *Chem. Commun.* **2002**, 2476. (b) Simonutti, R.; Bracco, S.; Comotti, A.; Mauri, M.; Sozzani, P. *Chem. Mater.* **2006**, *18*, 4651. (c) Springuel-Huet, M. A.; Guenneau, F.; Gédéon, A.; Corma, A. *J. Phys. Chem. C* **2007**, *111*, 5694.

(23) (a) Nossov, A.; Guenneau, F.; Springuel-Huet, M. A.; Haddad, E.; Montouillout, V.; Knott, B.; Engelke, F.; Fernandez, C.; Gédéon, A. *Phys. Chem. Chem. Phys.* **2003**, *5*, 4479. (b) Cheng, C. Y.; Bowers, C. R. *J. Am. Chem. Soc.* **2007**, *129*, 13997.

(24) Zhang, W. P.; Bao, X. H.; Guo, X. W.; Wang, X. S. *Catal. Lett.* **1999**, *60*, 89.

(25) (a) Chen, Q.; Springuel-Huet, M. A.; Fraissard, J.; Smith, M. L.; Corbin, D. R.; Dybowski, C. *J. Phys. Chem.* **1992**, *96*, 10914. (b) Zhang, W. P.; Han, X. W.; Liu, X. C.; Lei, H.; Liu, X. M.; Bao, X. H. *Micorporous Mesoporous Mater.* **2002**, *53*, 145.

(26) Sakthivel, A.; Huang, S. J.; Chen, W. H.; Lan, Z. H.; Chen, K. H.; Kim, T. W.; Ryoo, R.; Chiang, A. S. T.; Liu, S. B. *Chem. Mater.* **2004**, *16*, 3168.

(27) (a) Sears, D. N.; Demko, B. A.; Ooms, K. J.; Wasylishen, R. E.; Huang, Y. *Chem. Mater.* **2005**, *17*, 5481. (b) Knagge, K.; Smith, J. R.; Smith, L. J.; Buriak, J.; Raftery, D. *Solid State Nucl. Magn. Reson.* **2006**, *29*, 85.

(28) (a) Larsen, R. G.; Shore, J.; Schmidt-Rohr, K.; Emsley, L.; Pines, A.; Janicke, M.; Chmelka, B. F. *Chem. Phys. Lett.* **1993**, *214*, 220. (b) Moudrakovski, I. L.; Ratcliffe, C. I.; Ripmeester, J. A. *Appl. Magn. Reson.* **1995**, *8*, 385.